Magneto-optics in the Ultrafast Regime: Thermalization of Spin Populations in Ferromagnetic Films

Luca Guidoni,* Eric Beaurepaire, and Jean-Yves Bigot

Institut de Physique et Chimie des Matériaux de Strasbourg, Unité Mixte CNRS-ULP-ECPM, 23 rue du Loess, 67037 Strasbourg Cedex, France

(Received 30 November 2001; published 17 June 2002)

We have characterized by pump-probe polarimetry the time-dependent dielectric tensor in a $CoPt_3$ ferromagnetic film excited by 20 fs laser pulses. It is shown that, after the thermalization time of the electrons ($\simeq$50 fs), the dynamics of the real and the imaginary parts of the Voigt vector are identical. In addition, their relative variation is 10 times larger than that of the diagonal elements of the tensor, which allows one to infer that the spins dominate the magneto-optical response. During the thermalization process, the temporal behavior of the tensor elements opens new questions concerning the dynamics of the spins associated to a nonthermal electronic population in a ferromagnet.

DOI: 10.1103/PhysRevLett.89.017401 PACS numbers: 78.47.+p, 75.40.Gb, 78.20.Ls, 78.66.Bz

The application of femtosecond time-resolved techniques to magneto-optics opened the way to measure the magnetization dynamics on the subpicosecond temporal scale. In the case of ferromagnetic metals, several detection schemes have been developed: the third-order (i.e., pump-probe) magneto-optical (MO) effect [1–4], magnetization-dependent surface second harmonic generation (MSSHG) [5–7], and time- and spin-resolved two photon photoemission [8–10]. Femtosecond time resolution is achieved by inducing the demagnetization via the absorption of an ultrashort laser pulse. The example of the complete demagnetization induced by a laser pulse of 100 fs in $CoPt_3$ [3] indicates that the magnetization can be modified within the time window between the pump pulse and the heating of the phonons. In this extreme situation, where a total demagnetization occurs within the pulse duration, the interpretation is clear since the material switches to its opposite magnetic state when it is maintained in a static magnetic field with an amplitude slightly less than the coercive field. In the regime of weak perturbation, however, the interpretation of MO experiments is more ambiguous. A recent study on Cu/Ni/Cu wedges demonstrated that the dynamical evolution of the Kerr ellipticity and rotation does not coincide during the first hundreds of femtoseconds, breaking the proportionality between the magnetization and the Voigt vector that is the basis of linear magneto-optics [4]. Moreover, Regensburger and co-workers studied a Ni(110) surface and concluded that the time evolution of MSSHG is not necessarily the signature of magnetization dynamics: A MSSHG signal can be dominated by the dynamics of the charges [7]. On the other hand, from a theoretical point of view, Zhang and Hübner have demonstrated the possibility of a real demagnetization of nickel within a characteristic time shorter than 20 fs [11]. The ultrafast drop of MO signals could therefore be the very simple consequence of such a demagnetization.

In this Letter we present results obtained with a temporal resolution that allows us to clearly resolve the initial dynamics of the MO response, which changes with a characteristic time of $\simeq$50 fs. Moreover, we are able to distinguish between the contributions of the spin and the charge populations in the MO signals. This is achieved by carefully separating the dynamics of the diagonal and the nondiagonal elements of the time-dependent dielectric tensor.

The samples are thin films of $CoPt_3$ alloy directly grown on a (0001) oriented sapphire crystal without any metallic buffer or capping layer. They are made by sequential deposition at 690 K of one Co monolayer and three Pt layers. A total thickness of 21.5 nm has been measured *ex situ* by x-ray reflectometry at grazing incidence. Two types of samples have been studied: In the first case, a 147 nm thick dielectric protection layer of MgF_2 has been deposited to avoid oxidation; in the other case, the protection layer was absent but the time-resolved experiments have been performed within the 24 hours following the extraction of the sample from the ultrahigh-vacuum apparatus. The study of the two types of samples leads to identical results. The laser pulses of 20 fs duration are delivered by a Ti:sapphire oscillator with a repetition rate of 83 MHz and a central wavelength of 780 nm. The cross correlation of the two pulses (pump and probe) focused on 30 μm overlapping spots (see Fig. 1) gives a pulse duration of 22 fs. The pump/probe intensity ratio is $>$10:1 and the maximum available pump energy is 2 nJ/pulse. The simultaneous detection of the MO signals and of the differential transmission $\Delta T/T$ and reflection $\Delta R/R$ is obtained with the setup sketched in Fig. 1. Both the polar Kerr $\tilde{\Theta}_K = \theta_K + i\eta_K$ and Faraday $\tilde{\Theta}_F = \theta_F + i\eta_F$ complex polarization rotations are acquired simultaneously. A double-modulation technique is used with a mechanical chopping of the pump at 170 Hz and a photoelastic modulation (at 50 kHz) of the reflected and transmitted probe polarizations [4]. The transmitted and reflected probe intensities are measured with a differential detection scheme by two pairs of Si photodiodes. Several quantities are accessible. By lock-in amplification at 50 and 100 kHz, we measure η_K and θ_K (reflection) as well as η_F and θ_F

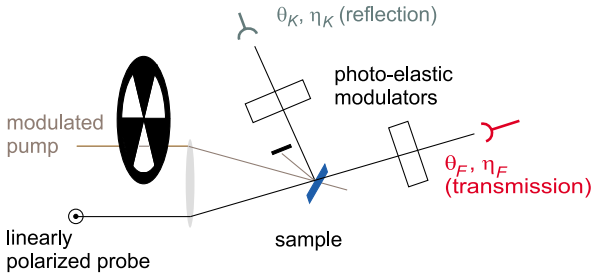

FIG. 1 (color online). Polarimetric detection scheme. The reflected (and transmitted) probe polarization state is measured with the double-modulation technique, the two photoelastic modulators being placed after the sample. The pump polarization can be changed between p, s, σ^+, or σ^-; the incident probe is s polarized.

(transmission). By a second stage of lock-in amplification referenced at 170 Hz of these four signals, we obtain their pump-induced variations $\Delta\eta_K$, $\Delta\theta_K$, $\Delta\eta_F$, and $\Delta\theta_F$. Finally, by direct lock-in amplification referenced at 170 Hz, we have access to the differential reflection and transmission ΔR and ΔT. The samples are studied in their remnant perpendicular magnetization state that can be reversed. The complex polarization rotations and their variations are obtained by taking the difference between the signals acquired for two opposite magnetization directions.

The linear static MO effect in a cubic magnetic medium, studied in the polar configuration, can be described by the first-order dielectric tensor,

$$\epsilon^{(1)} = \tilde{\epsilon}_{xx}\begin{pmatrix} 1 & i\tilde{Q} & 0 \\ -i\tilde{Q} & 1 & 0 \\ 0 & 0 & 1 \end{pmatrix}, \qquad (1)$$

where $\tilde{\epsilon}_{xx} = \epsilon'_{xx} + i\epsilon''_{xx}$ is the dielectric function and $\tilde{Q} = -i\tilde{\epsilon}_{xy}/\tilde{\epsilon}_{xx} = q' + iq''$ is proportional to the ratio of the nondiagonal and diagonal elements of $\epsilon^{(1)}$ [12]. The complex MO rotations $\tilde{\Theta}_K$ and $\tilde{\Theta}_F$, as well as the transmission T and reflection R of the sample, depend on $\epsilon^{(1)}$ and on the thickness of the film. In our case, we cannot neglect multiple reflections, so these quantities are numerically retrieved using a standard matrix method [13,14]. A subsequent differentiation allows us to extract the linear coefficients that relate the small variations of $\tilde{\epsilon}_{xx}$ to ΔT and ΔR [15,16]. By the same technique, the linear relationship between $\Delta\tilde{Q}$, $\Delta\tilde{\epsilon}_{xx}$, and $\Delta\tilde{\Theta}$ is also easily obtained. Our approach is therefore to extract from the pump-probe polarimetric experiment the dynamical evolution of the two independent complex variables $\tilde{\epsilon}_{xx}$ and $\tilde{Q}$. We stress that interpreting the experiment in terms of a temporal evolution of $\epsilon^{(1)}$ is different than considering a description in terms of third-order nonlinear polarization $P^{(3)}(t)$, which is the correct description in a pump-probe configuration. However, when the nonlinear polarization is dephased, one is justified in describing the nonlinear MO response in terms of a perturbation $\Delta\epsilon$ of the dielectric tensor $\epsilon^{(1)}$. This is true only because, after the electronic dephasing process has occurred ($t \gg T_2$), the contribution of the charges to the nonlinear response is isotropic. A consequence of this approximation is that no meaningful information can be extracted using this approach during the temporal overlap between the pump and probe pulses or during the characteristic electronic dephasing time T_2, which in a metal is shorter than 10 fs.

In Fig. 2 are shown the time-resolved differential transmission $\Delta T/T$ and reflection $\Delta R/R$ obtained with a p-polarized pump. We obtain a characteristic electronic thermalization time $\tau_{th} = 54 \pm 4$ fs and an electron-phonon interaction time $\tau_{e\text{-}ph} = 411 \pm 11$ fs by fitting the experimental data with the convolution of the pump pulse with a response function of the following form:

$$R(t) = H(t)\{K_1[1 - \exp(-t/\tau_{th})]\exp(-t/\tau_{e\text{-}ph}) + K_2[1 - \exp(-t/\tau_{e\text{-}ph})]\}, \qquad (2)$$

where $H(t)$ is the Heaviside function and $K_1 \gg K_2$. Such a response function can be derived by solving rate equations describing the energy transfer between thermal and nonthermal electronic populations and a phonon bath [17,18]. The short- and long-delay regions are well fitted by this function, as displayed in Figs. 2(a) and 2(b), respectively. The temporal evolution of the relative

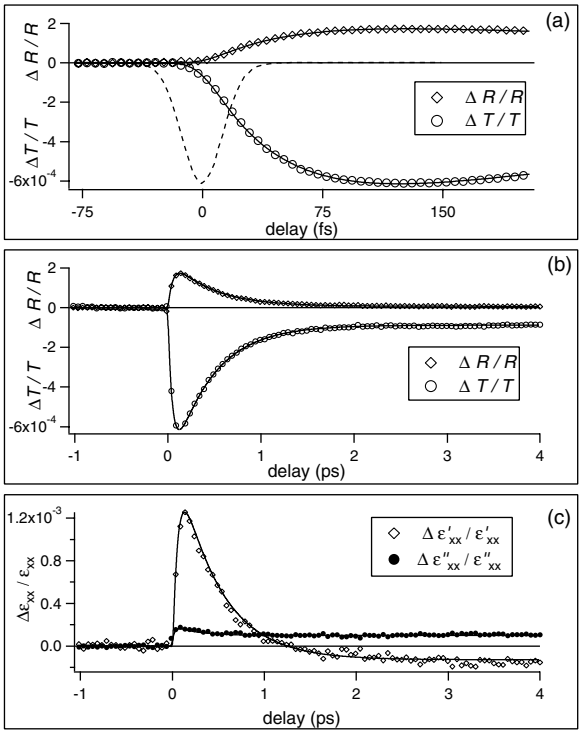

FIG. 2. Time-resolved differential transmission $\Delta T/T$ (∘) and reflection $\Delta R/R$ (◇) for short (a) and long (b) delays. The data are obtained with cross-polarized pump and probe and for a pump fluence of 100 μJ/cm^2. The solid line curves are the best fits with the response function $R(t)$ [Eq. (2)] convolved with a 22 fs pulse. The thermalization time $\tau_{th} = 54 \pm 4$ fs and the electron-phonon relaxation time $\tau_{e\text{-}ph} = 411 \pm 11$ fs are both obtained from the fit. (c) Temporal evolutions of the relative variations $\Delta\epsilon'_{xx}/\epsilon'_{xx}$ and $\Delta\epsilon''_{xx}/\epsilon''_{xx}$ of the real and the imaginary parts of the diagonal elements of the dielectric tensor as retrieved from the experimental results in (b).

variations of ϵ'_{xx} and ϵ''_{xx} are shown in Fig. 2(c). The quantitative description and understanding of this dynamical behavior would require an accurate knowledge of the band structure of the $CoPt_3$ alloy that is far beyond the scope of this paper. The important point for our purpose is that the maximum amplitude of the relative variations of ϵ'_{xx} and ϵ''_{xx} is of the order of 10^{-3} for a pump fluence of 100 μJ/cm^2.

The time-resolved MO signals acquired for the same pump fluence are shown in Fig. 3(a) for the long-delay range. These curves have been obtained by taking the difference between the two signals recorded with opposite directions of the remnant magnetization. Figure 3(b) shows the time evolution of the real and the imaginary parts of $\Delta\tilde{\epsilon}_{xy}$. These curves are retrieved by using the measured static values of $\tilde{Q} = 0.024 - i0.023$ and $\tilde{\epsilon}_{xx} = -16.4 + i37.0$ (at 780 nm).

Let us now discuss this dynamical behavior of the MO response. In the usual description of the linear static MO response, one writes the expression $\tilde{\epsilon}_{xy} = \tilde{\alpha}M$, where M is a real quantity [understood as the magnetization $M = \mu_B(N_{d\uparrow} - N_{d\downarrow})$, since mainly the d component of the magnetization is probed by magneto-optics], and $\tilde{\alpha} = \alpha' + i\alpha''$ is a complex quantity that contains the information about the electronic wave functions, the matrix elements associated with the spin-orbit interaction, and the coupling with the electromagnetic field [19]. A straightforward extension to the dynamical case is to differentiate the preceding expression, which gives

$$\Delta\epsilon'_{xy}/\epsilon'_{xy} = \Delta\alpha'/\alpha' + \Delta M/M,$$
$$\Delta\epsilon''_{xy}/\epsilon''_{xy} = \Delta\alpha''/\alpha'' + \Delta M/M.$$

Such a simplified expression is expected to be valid, as it is in the static case, as long as a thermal distribution of electrons can be assumed. This is the case of the long temporal delays displayed in Fig. 3 that we now discuss. As displayed in Fig. 3(b), the measured $\Delta\epsilon'_{xy}/\epsilon'_{xy}$ and $\Delta\epsilon''_{xy}/\epsilon''_{xy}$ have almost identical dynamics and, contrary to their diagonal counterparts, the same negative sign. Moreover, the amplitudes of $\Delta\epsilon'_{xy}/\epsilon'_{xy}$ and $\Delta\epsilon''_{xy}/\epsilon''_{xy}$ are 10 times larger than $\Delta\epsilon'_{xx}/\epsilon'_{xx}$ and $\Delta\epsilon''_{xx}/\epsilon''_{xx}$ [cf. Fig. 2(c)]. This behavior is easily understood if one assumes that the temporal variations of $\Delta\alpha'/\alpha'$ and $\Delta\alpha''/\alpha''$ have the same order of magnitude as the temporal variations of $\Delta\epsilon'_{xx}/\epsilon'_{xx}$ and $\Delta\epsilon''_{xx}/\epsilon''_{xx}$, which is a reasonable assumption considering that they both reflect the charge dynamics [20]. Therefore, we conclude that the curves displayed in Fig. 3 are *dominated by the time evolution of the spin populations.* Moreover, in this context, the quantities $\Delta q'/q'$ and $\Delta q''/q''$ should have the same dynamical behavior because they are both identified with $\Delta M/M$. This completely agrees with the retrieved $\Delta\tilde{Q}$ displayed in Fig. 3(c), which follow exactly the same dynamics for $t \gtrsim 150$ fs. Another important piece of information contained in Fig. 3 is that the long-delay temporal evolution of the nondiagonal elements of the dielectric tensor relaxes with almost the same constant $\tau_{e\text{-}ph}$ associated with the electron cooling to the lattice. This fact shows that for $t \gtrsim 150$ fs the spin dynamics is driven by the electronic temperature. Two scenarios can be invoked based on an unequal depopulation of the $d_\uparrow$ and $d_\downarrow$ bands $\frac{\Delta(N_{d\uparrow}-N_{d\downarrow})}{N_{d\uparrow}-N_{d\downarrow}} = \Delta M/M$, owing to the different density of states of $n_{d\uparrow}(E)$ and $n_{d\downarrow}(E)$ near the Fermi level. In the first case, an electronic transfer to the sp bands is assumed; no spin flips occur but part of the spin population is hidden from the point of view of the optical probe. The second scenario would allow for spin flips via the spin orbit coupling, a process which may occur with a characteristic time $\tau_{s\text{-}o} \simeq \hbar/E_{s\text{-}o} \simeq 1\text{–}5$ fs [21]. The spin relaxation would therefore be explained by a transfer between the spin and orbital components of the total magnetic moment. The first scenario relies on a thermal redistribution of electronic populations between the d and sp bands. Such a spectral anomaly has not been reported in the case of the CoPt alloy [21], which makes this interpretation less probable. In both cases, the electronic populations recover their initial spin polarization when they cool down to the lattice, implying a reversible spin dynamics.

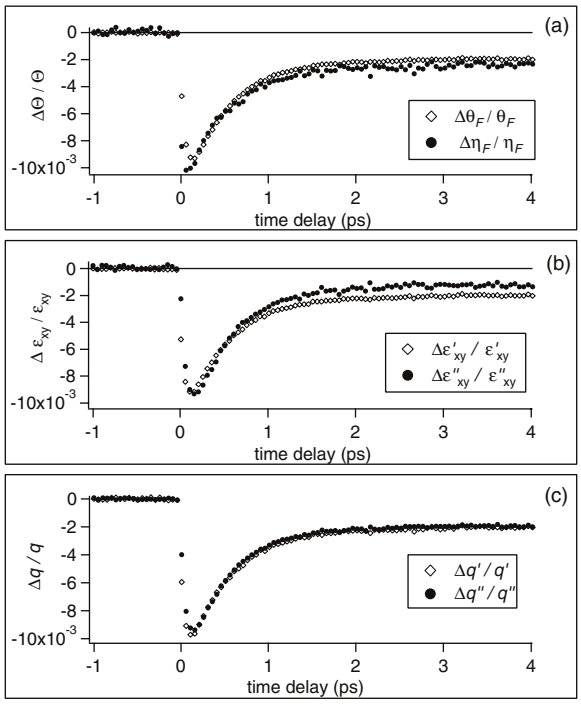

FIG. 3. (a) Time-resolved Faraday MO signals $\Delta\theta/\theta$ ($\diamond$) and $\Delta\eta/\eta$ ($\bullet$) for long temporal delays. (b) Temporal evolution of the real part [$\Delta\epsilon'_{xy}/\epsilon'_{xy}$ ($\diamond$)] and the imaginary part [$\Delta\epsilon''_{xy}/\epsilon''_{xy}$ ($\bullet$)] of the nondiagonal element of the dielectric tensor, retrieved from Faraday data. The equivalent Kerr-retrieved data (not shown) are perfectly consistent. (c) Temporal evolution of $\Delta q'/q'$ ($\diamond$) and $\Delta q''/q''$ ($\bullet$) also retrieved from data in (a). The fact that $\Delta q'/q'$ and $\Delta q''/q''$ follow exactly the same dynamics for $t \gtrsim 150$ fs shows that the residual difference between real and imaginary parts observed in (b) can be attributed to the (small) nonmagnetic contributions to the dynamics of nondiagonal tensor elements.

Let us now discuss the short-delay behavior of the MO response that is reported in Fig. 4, where the measured dynamics of $\Delta\tilde{\Theta}_F$ [4(a)] and the retrieved dynamics of $\Delta\tilde{Q}$ [4(b)] are shown. The initial spin population dynamics is related both to electron-electron scattering (which causes thermalization and could be a spin-dependent process) and to the spin-orbit interaction. Since these two effects have the same characteristic time scale, the simplified description of $\Delta\epsilon_{xy}/\epsilon_{xy}$ (that holds in the thermalized regime) will break down at short delays. As seen in Fig. 4(a), the time evolution of the real and imaginary parts of $\tilde{\Theta}_F$ is strongly different for short temporal delays ($t \lesssim 150$ fs). Such a behavior was already noticed in the paper by Koopmans and co-workers [4]. This difference can no longer be explained by the behavior of the diagonal elements of the tensor, as in the case of the thermalized regime. Indeed, in this regime, which we are able to identify unambiguously with the thermalization regime, the real and imaginary parts of $\Delta\tilde{Q}$ are also different [see Fig. 4(b) inset]. Therefore, the ultrafast loss in MO contrast (contrast that can be attributed to spin populations, in view of the long-temporal-delay results) is associated with the thermalization of spins. These results raise the question of which formal description should be used to account for the spin dynamics during the thermalization process.

In conclusion, we have studied the MO response of the $CoPt_3$ alloy grown on a sapphire substrate with pump-probe polarimetric experiments performed with 20 fs pulses. The analysis of a complete set of measurements, both static and time-resolved, allows us to retrieve and compare the respective contributions to the MO signals of the diagonal and nondiagonal elements of the dielectric tensor. Such analysis demonstrates that an ultrafast spin dynamics occurs during the thermalization of the electronic populations with a characteristic time of about 50 fs. This process is followed by a quasistatic equilibrium where the spins follow the dynamics of the electronic temperature.

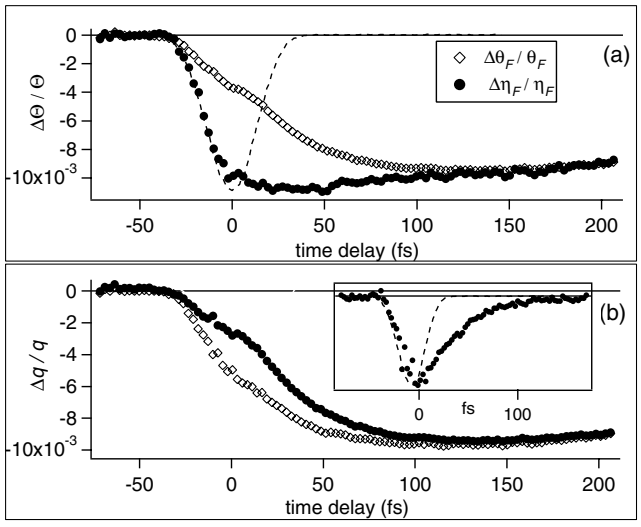

FIG. 4. (a) Time-resolved Faraday MO signals $\Delta\theta/\theta$ ($\diamond$) and $\Delta\eta/\eta$ ($\bullet$). The pump-probe cross correlation (dashed line) is displayed for reference. (b) Short-delay relative variations of $\Delta q'/q'$ ($\diamond$) and $\Delta q''/q''$ ($\bullet$) retrieved from the data in (a). For $t \lesssim 150$ fs, the real and the imaginary parts of $\Delta\tilde{Q}$ follow clearly different dynamics. The difference between $\Delta q'/q'$ and $\Delta q''/q''$ is plotted in the inset.

We thank J.-C. Merle and O. Cregut for helpful discussions, D. Acker for technical support, and J. Arabski, G. Schmerber, and F. Huber for sample preparation and characterization.

*Email address: Luca.Guidoni@ipcms.u-strasbg.fr

[1] E. Beaurepaire, J.-C. Merle, A. Daunois, and J.-Y. Bigot, Phys. Rev. Lett. **76**, 4250 (1996).
[2] G. Ju, A. Vertikov, A. V. Nurmikko, C. Canady, G. Xiao, R. F. C. Farrow, and A. Cebollada, Phys. Rev. B **57**, R700 (1998).
[3] E. Beaurepaire, M. Maret, V. Halté, J.-C. Merle, A. Daunois, and J.-Y. Bigot, Phys. Rev. B **58**, 12 134 (1998).
[4] B. Koopmans, M. van Kampen, J. T. Kohlhepp, and W. J. M. de Jonge, Phys. Rev. Lett. **85**, 844 (2000).
[5] J. Hohlfeld, E. Matthias, R. Knorren, and K. H. Bennemann, Phys. Rev. Lett. **78**, 4861 (1997).
[6] J. Güdde, U. Conrad, V. Jähnke, J. Hohlfeld, and E. Matthias, Phys. Rev. B **59**, R6608 (1999).
[7] H. Regensburger, R. Vollmer, and J. Kirschner, Phys. Rev. B **61**, 14 716 (2000).
[8] A. Scholl, L. Baumgarten, R. Jacquemin, and W. Eberhardt, Phys. Rev. Lett. **79**, 5146 (1997).
[9] M. Aeschlimann, M. Bauer, S. Pawlik, W. Weber, R. Burgermeister, D. Oberli, and H. C. Siegmann, Phys. Rev. Lett. **79**, 5158 (1997).
[10] R. Knorren, K. H. Bennemann, R. Burgermeister, and M. Aeschlimann, Phys. Rev. B **61**, 9427 (2000).
[11] G. P. Zhang and W. Hübner, Phys. Rev. Lett. **85**, 3025 (2000).
[12] In the static measurements $\tilde{Q}$, usually named "magneto-optical constant," characterizes the strength of the MO response. See, for example, G. Metzger, P. Pluvinage, and R. Torguet, Ann. Phys. (Paris) **10**, 5 (1965).
[13] F. Abelès, in *Advanced Optical Techniques,* edited by V. Heel (North-Holland, Amsterdam, 1967), p. 144.
[14] J. Zak, E. R. Moog, C. Liu, and S. D. Bader, Phys. Rev. B **43**, 6423 (1991).
[15] R. Rosei and D. W. Lynch, Phys. Rev. B **5**, 3883 (1972).
[16] C. K. Sun, F. Vallée, L. H. Acioli, E. P. Ippen, and J. G. Fujimoto, Phys. Rev. B **50**, 15 337 (1994).
[17] R. W. Schoenlein, W. Z. Lin, J. G. Fujimoto, and G. L. Eesley, Phys. Rev. Lett. **58**, 1680 (1987).
[18] N. Del Fatti, C. Voisin, M. Achermann, S. Tzortzakis, D. Christofilos, and F. Vallée, Phys. Rev. B **61**, 16 956 (2000).
[19] P. N. Argyres, Phys. Rev. **97**, 334 (1955).
[20] This assumption is verified in the simple case of the Lorentz model of a bound electron in a magnetic field, with the exception of some particular resonant situations which are not relevant in our case. See, for example, W. Voigt, *Magneto- und Electro-Optik* (Teubner, Leipzig, 1908).
[21] L. Uba, S. Uba, V. N. Antonov, A. N. Yaresko, and R. Gontarz, Phys. Rev. B **64**, 125105 (2001).